Eur. Phys. J. D **6**, 441–450 (1999)

THE EUROPEAN
PHYSICAL JOURNAL D
EDP Sciences

Triply excited three-electron systems—semiclassical model

P.V. Grujić[a]

Institute of Physics, P.O. Box 57, 11000 Belgrade, Yugoslavia and Faculty of Physics, P.O. Box 550, 11000 Belgrade, Yugoslavia

Received: 16 September 1998 / Received in final form: 16 March 1999

Abstract. We calculate rovibronic intrashell spectra of the triply highly excited atomic hydrogen dianion, helium anion and lithium atom, within a simple semiclassical model. Zero-order electronic energy levels and half-lives are calculated for a number of principal quantum numbers and approximate thresholds for the appearance of vibronic modes are estimated. Since no quantum-mechanical and experimental data are available for the highly excited levels ($N > 5$), where the semiclassical models apply, no comparison with other results are possible at present. The problem of comparing semiclassical and quantum-mechanical calculations for moderately large quantum numbers, which seem attainable by the present day experimental technique, has been discussed.

PACS. 31.50.+w Excited states – 31.25.Jf Electron-correlation calculations for atoms and ions: excited states

1 Introduction

Multiply excited atoms have been the subject of intense investigations in the last three decades, for they exhibit most explicitly inter-electron correlation effects. In particular, doubly excited states have been widely used as a means of demonstrating the crucial role of electron correlation. In recent years we witness a shift towards triply and even quadruply excited systems, where the correlation effects are even more pronounced.

Watanabe and Lin [1] classified possible triply excited states as isomorphic to molecular D_{3h} symmetry. Their model was restricted to the intrashell states, more precisely to the model with three electrons on a sphere. A number of possible bending modes was identified and the energy levels grouped into manifolds resembling the rotational structure of a symmetric top. In a series of papers Bao and collaborators have analyzed a number of model triply excited states (see [2] and references therein), within the quantum-mechanical approach. In [3] possible modes of internal motions in a model system of the $^2S^e$ states have been analyzed. In the model radial modes are suppressed and possible configurations within the same shell are examined. It turns out that three co-plane structures dominate the triply excited configurations: (irregular) triangle, the straight rod and the sharp wedge (see Fig. 4a-c in [3]). If all three electrons have parallel spins, as in $^4S^o$ state, plane structure appears again, among others possible configurations, this time as a equilateral triangle [4]. Since, however, all electrons have the same principal and angular momentum quantum numbers, they are forced to oscillate through the plane (see Fig. 4 in [4]). This model corresponds to what is known from the early semiclassical theory of two-electron system as Langmuir's oscillatory model (see *e.g.*, [5–7] and references therein). These papers have clarified the important issue of the internal degrees of freedom and possible classification schemes. Further symmetry effects have been analyzed in [8] for low-lying intrashell states, within coplanar configurations. It should be stressed that all above qualitative studies have used *ad hoc* classical geometries of the relevant atomic states.

All concrete calculations carried out so far have been applied to relatively low excited states, within the quantum-mechanical approach. Resonances in He$^-$ within Feshbach projection formalism have been studied by Bylicki [9], who calculated the energy of $2s^22p\,^2P^o$ and $2s2p^2\,^4P^e$ states, which are situated just above the double ionization threshold. For the former state the calculated energy is $E = -0.80154\,\text{au}$. Nicolaides *et al.* developed a general *ab initio* method for treating multiply (triply, quadruply etc.) excited (resonant) states [10]. They used square-integrable functions for the so-called open-channel–like correlating configurations, which go beyond the standard Feshbach theory. They found a number of new triply excited states, like $2s2p^2\,P$ and $2p^3\,^2D^o$, which appear above both singly and doubly excited configurations. Triply excited states abound in electron-atom scattering and are measured by many authors, but the identification of these usually mutually very close states is not straightforward (see,*e.g.*, [10] and references therein). Komninos and Nicolaides have extended these calculations to the quadruply excited atoms [11], finding that as the fourfold ionization threshold is approached the $^5S^o$ states tend to assume the tetrahedral structure. Taken together with earlier *ab initio* calculations findings for double

---

[a] e-mail: `grujic@phy.bg.ac.yu`

(linear, Wannier-ridge configuration, see, *e.g.*, [12]) and triple (equilateral triangle) ionization ladders (see, also, *e.g.*, [1,13]) it turns out that in the limit of the total fragmentation threshold multiply excited states follow the most symmetrical configurations. These findings, in turn, corroborate earlier conjectures that there is a strong symmetry across the total ionization threshold regarding the small-energy Coulombic systems, based on the classical dynamics considerations [14].

We mention also theoretical works by Bachau [15] on $(n = 3)$ triply excited states of multicharged ions and by Gou and Chung [16] on the triply excited lithium-like ions.

Semiclassical theory has passed a long way from Bohr's Old Quantum theory to the present-day status. As noted by Percival and collaborators [5,17] the failure to describe few-electron atoms, notably helium, should be attributed, what now has been realized, to improper quantization rules. These have been elucidated by Einstein and other authors and the present state of affairs has been fairly well represented by EBK (Einstein-Brillouin-Keller) theory. The very application of the semiclassical methods, however, is still less straightforward than the case with the quantum-mechanical calculations. It is in order here to compare both approaches regarding the practical applications in atomic physics.

Quantum-mechanics. i) Exact results: two-body Coulomb systems (hydrogen-like atoms, etc.), linear harmonic oscillator; ii) accurate analytical and numerical results: three-body systems (helium atom, H_2^+, etc.); iii) approximate analytical methods: four-body and higher-order atomic systems (lithium, H_2, etc.).

Semiclassical theory (spin variable usually ignored). i) Exact results: the same as for quantum mechanics (correspondence identities) [18,19]; ii) accurate results: same as for quantum mechanics, but only for large relevant quantum numbers (correspondence principle) [17]; iii) approximate results—same as for quantum mechanics.

A proper application of the semiclassical theory has greatly improved the accuracy of the ground-state helium (nonrelativistic) calculations [5]. As for the doubly excited two-electron systems, the literature is abundant and we refer the interested reader to review articles (*e.g.*, [20,21]). Two general remarks, however, about the applicabilities of the two approaches seems in order here. First, quantum-mechanical calculations are limited by our mathematical (in)abilities only, whereas the semiclassical methods must rely heavily on a suitable choice of the model. The latter means that a relevant choice of the underlying classical configuration must be made, since usually the aim of including all possible classical paths appears beyond our reach. Second, quantum treatments are feasible for the low-lying states only, whereas the semiclassical calculations are expected to yield good results for highly excited states. In this sense two approaches are complementary. The principal aim (and difficulty) appears thus the intermediate region of moderately excited states, with not too large quantum numbers. For it is this region where the validity of the semiclassical approach appears questionable and should be tested by the quantum-mechanical calculations. The latter appear, in their turn, very cumbersome even for the low-lying states and the comparison is not easy to achieve. Generally, this intermediate region lies within the $n^* = 5$–8 span, where n^* is the smallest effective principal quantum number ascribed to individual system constituents. Another hindrance to the comparison of semiclassical and quantum-mechanical results in this region is the empirical fact that the latter calculations are made, as a rule, for the low total angular momentum values (these are, usually, S-states). These quantum-mechanical electron configurations are the furthest from the semiclassical ones, which involve generally large total angular momenta. The reason for the latter is that not only that large quantum numbers are required for the semiclassical approach, but the electron correlation effects, which are crucial for ensuring the configuration stability, demand "coherent addition" of the individual momenta. It is this requirement which forces the three-electron systems either to remain in plane (coplanar case), or to oscillate in phase through the plane [4].

The study of negative ions has both practical and conceptual importance. In the case of the simplest system, H^{2-}, there appears the existence problem, which has not yet been solved in a satisfactory manner (see, *e.g.*, [22, 23], and references therein). Hydrogen dianions have recently attracted much attention both experimentally [24, 25] and theoretically [27,29] (see, also recent paper [26] on the general problem of maximal electronic charge bound by atomic nuclei, and references therein). The problem as to the possible existence of these dianions, either as stable or transient systems, does not seem to be settled down. Early observations in the $e + H^-$ scattering indicated the presence of H^{2-} resonances and a quick theoretical calculations corroborated these experimental findings (see, *e.g.*, [28] and references therein). Subsequent theoretical investigations, however, alternated between positive [27], and negative [29,30] conclusions. However, the very recent complex coordinate rotation calculations reveal the existance of at least two resonance states [22].

As for the (metastable) helium anion, with its small electron affinity $I = 0.076\,\mathrm{eV}$ (He$[1s2s2p]$), electron scattering processes appear abundant in the resonance states. These are, however, mostly doubly excited states, which have been the subject to numerous investigations, both experimental and theoretical (see, *e.g.*, [31] for the low-lying and [32] for highly excited states, and references therein). The situation is even less favourable with the lithium atom with regard to the multiply excited states, though a number of experimental and theoretical investigations have been recently reported (*e.g.*, [33]).

All those theoretical and experimental studies were mainly concerned either with the ground, or low-lying excited states. As the quantum-mechanical calculations mentioned above indicate, multiply excited states tend to acquire highly symmetric structures, with many degrees of freedom suppressed, which make them close to single electron configurations. This implies that only global features of highly excited states are both discernable and relevant. All these properties make these states amenable to the semiclassical theory. Here we investigate the triply highly excited states within the semiclassical approach, and examine the physical properties of such a model. We carry out semiclassical investigations of the possible intrashell H^{2-}, He^{-} and lithium states, within the so-called coplanar model. In the next section we set up the classical three-electron model and in Section 3 calculate the energy spectrum and the corresponding lifetimes of the states. In the final Section 4 we discuss the model and its further prospects in describing few-electron systems.

2 The classical model—coplanar case

In [35] the semiclassical theory of highly excited three-body atomic systems was applied in evaluating the rovibronic spectra, including that of two-electron excitations. Here we extend these calculations to the three-electron system, which belongs to the quasi–four-body problem. As is usual in setting up a semiclassical model, one starts with a class of supposed underlying classical configurations and then applies a relevant quantization procedure to extract energy levels and other associated quantities. As mentioned above, the number of these classes can be large even for the simpler two-electron systems. One has to restrict himself to a class which appears sufficiently generic and at the same time simple enough as to allow feasible calculations. As mentioned above, these configurations are endowed with some high symmetry. Plane configurations are the first to satisfy these requirements.

This approach parallels, in fact, that of the quantum-mechanical configuration interaction (CI) method, which, in principle, should include an infinite number of bound and continuum states for an accurate result. Singling out one of all possible classical configurations corresponds to retaining only one of the quantum-mechanical electron configurations (that one is calculating), ignoring the coupling to other configurations (configuration mixing). For the highly excited states we know that the number of neighbouring states (levels) appears enormous and the standard quantum-mechanical approach would require a prohibitive (both analytical and computational) time. Fortunately, this complication appears advantageous once one passes to the (semi)classical picture. For we know that it is a superposition of many neighbouring states which gives rise to forming a wave packet, which travels along a Keplerian orbit, in the Coulomb case (see, *e.g.*, [36] and references therein).

Within this approach all electrons are treated on an equal footing, which implies a choice of a configuration endowed with maximum symmetry in the configuration space. For the case at hand it amounts to the choice of the equilateral triangle geometry, as shown in Figure 1, for the plane case.

If the nucleus charge is Z, each of the electrons sees an effective charge $Z_{\text{eff}} = Z - 1/\sqrt{3}$ at the origin and moves along a Keplerian orbit, always staying at the vertex of an equilateral triangle. The latter rotates and shrinks/expands as the electrons follow the elliptic orbits around the centre of mass. The maximum angular momentum of the single electron is $\ell_{\max} = \sqrt{-2E/3}$, where E is the total energy of the system ($E = 3\epsilon$). This corresponds to the motion along the common circle, the case studied already by Bohr within the Old Quantum theory. The latter is known to have yielded wrong quantized energy levels for He and was quickly abandoned, as well as Sommerfeld's generalization to the $\ell < \ell_{\max}$ (elliptic orbits). However, it is well established now that the Old Quantum i) could not provide exact results for the ground state in principle and ii) the theory failed to yield reasonably accurate answers mainly because of the applied inappropriate quantum conditions (see, *e.g.*, [19,5]).

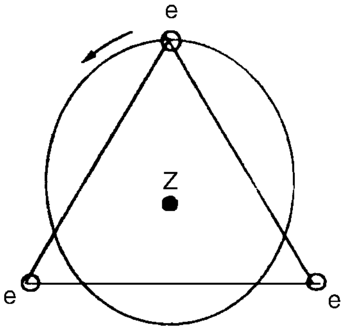

Fig. 1. 2D configuration for the three-electron intrashell state (schematic). Only one of three Keplerian orbits is shown.

Here, we consider Bohr's circular configurations first. If the total angular momentum is $\mathcal{L}$, then one has (Lande's rule)

$$\mathcal{L} = L + \frac{1}{2}, \quad L = 0, 1, 2, \ldots, L_{\max}. \tag{1}$$

We calculate the potential for the hydrogen anion, for the sake of illustration. Let the total energy of H^{2-} be $E = -0.063$ au, as computed by Sommerfeld *et al.* [27]. The effective potential attributed to the single electron is then

$$V_{\text{eff}} = -\frac{Z_{\text{eff}}}{r} + \frac{\left(L + \frac{1}{2}\right)^2}{18r^2}, \quad Z_{\text{eff}} = 0.42265 \quad (Z = 1). \tag{2}$$

The potential function is shown in Figure 2 for $\mathcal{L} = 6.233$. Imposing that the potential minimum equals the single-electron energy ϵ, one finds the corresponding parameters,

$$\ell = \ell_{\max} = 2.078\,\text{au}, \quad r_{\text{eq}} = \frac{\left(L + \frac{1}{2}\right)^2}{9Z_{\text{eff}}}. \tag{3}$$

For the case at hand one has $r_{\text{eq}} = 10.22\,a_o$ ($L = 5.733$ in Eq. (1)). (We note that the strict implementation of the quantization conditions (1) provides for the ground state level ($L = 0$) $E = -9.63$ au! The semiclassical model is

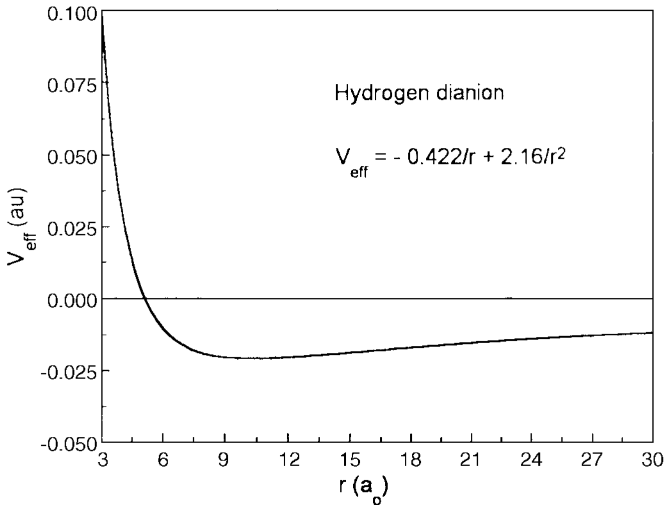

Fig. 2. Effective potential for a single electron in H^{2-} from equation (2), for $\mathcal{L} = 6.233$.

valid for large L values and is inappropriate, as expected, to describe the H^{2-} anion low-energy spectrum.)

For the noncircular orbits, one applies the general quantization conditions (*e.g.*, [17])

$$\oint p_r \mathrm{d}r = 2\pi \left(n_r + \frac{1}{2} \right), \quad n_r = 0, 1, 2, \dots, \tag{4}$$

$$\oint p_\theta \mathrm{d}\theta = 2\pi \left(\ell - m + \frac{1}{2} \right), \quad \ell = 0, 1, \dots, n_r, \tag{5}$$

$$\oint p_\phi \mathrm{d}\phi = 2\pi m, \quad |m| = 0, 1, \dots, \ell. \tag{6}$$

For the motion in plane, $m = 0$ and one has

$$p_r = \sqrt{2(\epsilon - V) - \ell^2/2r^2}, \quad V = -\frac{Z_{\text{eff}}}{r}, \quad \ell = \frac{L + 1/2}{3}, \tag{7}$$

so that (4) reads (see Fig. 2)

$$\int_{r_p}^{r_a} \sqrt{2\left(\epsilon + \frac{Z_{\text{eff}}}{r}\right) - \frac{L + 1/2}{18r^2}} = \pi(n_r + 1/2), \tag{8}$$

with perihelion and aphelion distances given by (e is the orbit eccentricity, μ the reduced mass)

$$r_{\mathrm{p}} = \frac{\ell^2}{1+e}, \; r_{\mathrm{a}} = \frac{\ell^2}{1-e}, \; e = \sqrt{1 + 2\ell^2\epsilon/\mu}, \; \ell = \frac{L + 1/2}{3}, \tag{9}$$

We note that noncircular orbits ($\ell \le \ell_{\max}$) do not provide anything new, as far as the energy spectrum is concerned, since the energy is independent of the angular momentum (for this symmetry!), because of the so-called accidental degeneracy. Further, for large principal quantum numbers $n_1, n_2, n_3 = n \gg 1$ and the biggest possible angular momenta $\ell_1, \ell_2, \ell_3 = n - 1$, elliptical orbits will appear practically indistinguishable from the circular ones. Thus, we proceed with the circular electron orbits.

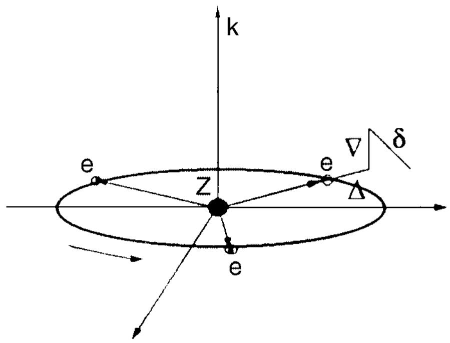

Fig. 3. Three-electron system configuration (see text). The rotation axis is along the **k** vector).

We ignore the spin of particles, both as a quantum-mechanical and dynamical variable. The former enters the stage *via* Pauli's exclusion principle, which in our case would forbid strictly symmetrical configurations, or equivalently the identical sets of quantum numbers (n, ℓ, m). However, for large values of n, ℓ ($m = 0$ in our case) relatively small deviations (like $\ell_1 = \ell_2 - 1$) would circumvent the problem, still providing practically the same classical configurations. As for the dynamical effects, like the spin-spin interaction, which in the classical approach results in small deviations from the trajectories calculated in purely Coulombic potential, these effects are negligibly small as long as the electrons are close to the equilibrium positions, which for the large angular momenta are well separated in space (see Eq. (9)). Thus we shall ignore all terms in the Hamiltonian which involve dipole-monopole, dipole-dipole, etc. interactions.

Besides the rotational motion the three-electron system has additional degrees of freedom, deviations from the corresponding equilibrium positions. If these deviations are small, one can evaluate the rovibronic spectrum for this circular configuration, as it was done for the two-electron case [37]. Let all three electrons be situated at the vortices of an equilateral triangle, as shown in Figure 3, lying in XOY plane.

In analyzing the classical underlying configurations we make use of the properties of the same systems in the continuum, *i.e.* for small, positive total energies. As discussed above, few-electron system configurations close to the total fragmentation threshold exhibit many common features. In both cases electrons tend to assume the most (possible) symmetrical configurations, thus minimizing the system potential energy function on the constant hyperradius sphere. In the near-threshold ionization case angular motion is suppressed and the radial mode appears to be the dominant one. On the contrary, in the bound-state case the radial mode is suppressed for the small Keplerian orbit eccentricities, while the lateral motion dominates (see, *e.g.*, [14]).

Let the whole system rotate around the OZ-axis, so that the centrifugal force balances the net Coulomb force. We displace all electrons from this (leading) configuration, by writing in the rotating frame of reference (we disregard here the coupling between rotational and vibrational motions, *i.e.* the Coriolis force, cf., *e.g.*, [38,39]):

$$\mathbf{r}_i = (r_i^{(0)} + \varDelta)\mathbf{n}_r + \delta \mathbf{n}_\phi + \nabla \mathbf{k}, \quad \varDelta, \delta, \nabla \ll r, \tag{10}$$

where **n** and **k** are unit vectors in the corresponding directions. We consider the kinematics of small variations, by inserting equation (10) into Newton's equations for the electrons in the field of an infinitely heavy charge Z:

$$\frac{\mathrm{d}^2\mathbf{r}_i}{\mathrm{d}t^2} = \sum_{i \neq j} \frac{\mathbf{r}_{ij}}{r_{ij}^3} - Z\frac{\mathbf{r}_i}{r_i^3}, \quad i, j = 1,\, 2,\, 3\,. \tag{11}$$

At fixed $r_i^{(0)} \equiv r$ one obtains for the small deviations the matrix equation (see [37])

$$\mathbf{D}^2\mathbf{IF} = \mathbf{BF}, \quad \mathbf{D}^2 \equiv r^3 \frac{\mathrm{d}^2}{\mathrm{d}t^2}, \tag{12}$$

where **I** is the unit matrix, **F** is the column vector

$$\mathbf{F} = \{\varDelta_1, \varDelta_2, \delta_1, \delta_2, \nabla_1, \nabla_2\}^{\mathrm{T}}, \tag{13}$$

where T denotes the row transposition and

$$\mathbf{B} = \left\{ \begin{matrix} b_1 & 0 & -\frac{1}{12} & -\frac{1}{6} & 0 & 0 \\ 0 & b_1 & \frac{1}{6} & \frac{1}{12} & 0 & 0 \\ \frac{1}{12} & \frac{1}{6} & b_2 & 0 & 0 & 0 \\ -\frac{1}{6} & -\frac{1}{12} & 0 & b_2 & 0 & 0 \\ 0 & 0 & 0 & 0 & -Z & 0 \\ 0 & 0 & 0 & 0 & 0 & -Z \end{matrix} \right\}, \tag{14}$$

$$b_1 = 2Z - \frac{1}{4\sqrt{3}}, \quad b_2 = -\left(Z + \frac{1}{4\sqrt{3}}\right). \tag{15}$$

Solutions for ∇ deviations of equation (12) can be written as

$$\begin{aligned} \nabla_j &= \nabla = C_\theta^{(1)} e^{i\omega_\theta t} + C_\theta^{(2)} e^{-i\omega_\theta t}, \\ \omega_\theta &= \frac{\sqrt{\lambda_\theta}}{r_{\mathrm{eq}}^{3/2}}, \quad \lambda_\theta \equiv Z, \quad j = 1, 2, 3, \end{aligned} \tag{16}$$

where $C_\theta^{(i)}$ are arbitrary constants.

For the in-plane deviations one has to diagonalize the corresponding 4×4 submatrix of **B** from equation (12). This, however, is not easy to achieve, since the corresponding secular equation has two pairs of double roots,

$$\lambda_{1,2} = \frac{1}{2}\left[Z - \frac{1}{2\sqrt{3}} + \sqrt{9Z^2 + \frac{1}{12}}\right], \tag{17}$$

$$\lambda_{3,4} \equiv \lambda_\phi = \frac{1}{2}\left[Z - \frac{1}{2\sqrt{3}} - \sqrt{9Z^2 + \frac{1}{12}}\right]. \tag{18}$$

However, as calculations for the equivalent problem of the triple escape at small electron energies have shown [37], the exact (after diagonalization) values differ marginally from the zero-order approximation, *i.e.* when the (small) off-diagonal elements are ignored. An inclusion of these off-diagonal elements would result in the mixed terms appearance, which spoil the distinction between stable (vibronic) and unstable (radial) motions. Thus, lateral electron motion would acquire a (small) unstable mode admixture, whereas the radial mode would include a small vibrational component.

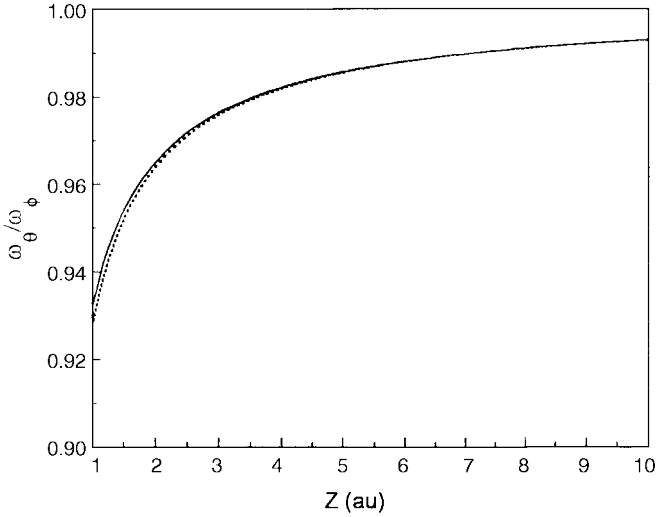

Fig. 4. Vibronic angular frequences ratio. Full curve: the exact formula (21); dashed curve: the approximate expression (22).

Hence, one has for the small deviations in the plane:

$$\begin{aligned} &\varDelta_j = \varDelta = C_r^{(1)} e^{\lambda_r t} + C_r^{(2)} e^{-\lambda_r t}, \quad \lambda_r = \frac{\sqrt{\lambda_1}}{r_{\mathrm{eq}}^{3/2}}, \\ &j = 1, 2, 3, \end{aligned} \tag{19}$$

$$\begin{aligned} &\delta_j \equiv \delta = C_\phi^{(1)} e^{i\omega_\phi t} + C_\phi^{(2)} e^{-i\omega_\phi t}, \quad \omega_\phi = \frac{\sqrt{-\lambda_\phi}}{r_{\mathrm{eq}}^{3/2}}, \\ &j = 1, 2, 3, \end{aligned} \tag{20}$$

where $C^{(i)}$ are arbitrary constants. From equations (17,20) one has

$$\left(\frac{\omega_\theta}{\omega_\phi}\right)^2 = \frac{2Z}{\dfrac{1}{2\sqrt{3}} + \sqrt{9Z^2 + \dfrac{1}{12}} - Z}, \tag{21}$$

so that one has an approximate estimate:

$$\left(\frac{\omega_\theta}{\omega_\phi}\right)^2 = \frac{1}{8Z\sqrt{3}}\,. \tag{22}$$

In the large-Z limit both frequencies merge and one has a degenerate case, when electrons move along circular orbits, around the equilibrium positions, in the rotating reference system. This is to be compared with two-electron systems, when the degeneracy appears at any Z, and the three-body system can be considered performing rotational motion around an axis in the XOY plane, which in its turn rotates around the OZ-axis (see [37] and references therein). In Figure 4 we plot the exact ratio function (21) and the approximate expression (22), as a function of the nucleus charge Z. One can see that the near-degeneracy is attained even at the smallest $Z = 1$ value (0.9278).

3 Rovibronic spectra calculations

Before we proceed with calculations, we estimate the region of applicability of our first-order perturbation method. To ensure the harmonicity conditions (see Eq. (10)) we require that the oscillation amplitudes remain small compared with the common radius of the orbits. One can estimate this amplitude by equating the harmonic oscillator energy with the potential energy at the turning point ($r = a$):

$$\frac{1}{2}ka^2 = \left(m + \frac{1}{2}\right)\omega, \quad k = \omega^2, m = 0, 1, 2, \ldots. \tag{23}$$

From equation (3) one has for $a \ll r_{\text{eq}}$ the (approximate) harmonicity condition, accounting for equations (17,20):

$$L + \frac{1}{2} \ggg 6\sqrt{\frac{\frac{1}{\sqrt{3}} - Z}{\lambda_{\phi,\theta}}}\left(m + \frac{1}{2}\right), \; m = 0, 1, 2, \ldots, \tag{24}$$

where $\ggg$ means larger by two orders of magnitude. As one can infer from equation (19), motion along the r-coordinate appears unstable and small initial deviations from the equilibrium positions grow exponentially in time. In the near-threshold problem it is this instability that determines the threshold law (see, *e.g.*, [37]). In the bound-state case, λ_r plays the role of Lyapunov exponent (cf., *e.g.*, [40] for the two-electron case), and is inversely proportional to the half-time τ of the excited level (cf., *e.g.*, [41]):

$$\tau = \frac{\ln 2}{\lambda_r}. \tag{25}$$

From equations (3) and (19) one sees that the Lyapunov exponents diminish as the level is more excited, so that the stability of the orbit (and consequently the half-life τ) increases. This is the general result for multiply excited states (see, *e.g.*, [42] and references therein; cf. also [43, 32]). Also, from equations (3,16) and (25) one has for the level half-widths

$$\Gamma \sim \frac{1}{n^3}, \quad L_{\max} \approx n \gg 1, \tag{26}$$

that is in accordance with earlier findings for doubly excited states [41] (but see also [44]).

One can quantize the corresponding energy levels by making use of the (implicit) formula due to Miller [45]:

$$\mathcal{E} = S^{-1}\left[2\pi(n + \lambda/4)\right] + \sum_{i=1}^{n-1}(m_i + \tfrac{1}{2})\hbar\omega_i(\mathcal{E}),$$
$$n = 1, 2, \ldots, \quad m_i = 0, 1, 2, \ldots, \tag{27}$$

where (operator) S is the action along a periodic orbit, and λ is the number of turning points on the orbit. If T is the period, $\nu_i = \omega_i T$ is the so-called stability index, where ω_i are the normal-mode oscillation frequencies, around the periodic orbit. The first member in (27) corresponds to the n-kvanta energy along the orbit, while each member of the sum represents the energy of m_i kvanta in i-th normal mode perpendicular to the orbit. Formula (27) is exact in the case of separable systems, if the oscillations around the orbit are harmonic. We note here that formula (27) disregards the intermode coupling too (see above).

Before presenting specific results, a few remarks are in order. Besides the general remark that the experimental evidence and theoretical calculations are still confined to the low-lying excited states, there is the additional problem of identifying states to be compared with the semiclassical calculations. As shown in the case of double excitations, the standard independent-particle picture fails and new, more appropriate state designations (that is, sets of quantum numbers) have been adopted (see, *e.g.*, [1] and references therein). In the case of triple excitations, attempts to devise similar classification schemes have been made, but up to now the situation is not yet as advanced as the case with double excitation is. What one encounters with the quantum-mechanical and experimental results is a mixture of usually large number of the independent-particle configurations, associated with particular energy levels. On the other hand, semiclassical states appear pure states from the quantum-mechanical point of view.

A number of the classification schemes proposed by some authors, within the quantum-mechanical theory, is restricted to the electrons situated on a sphere, as mentioned in the introduction. While this approach is useful in the qualitative analysis, it is not a realistic representation of the actual physical situation. Our model deals also with electrons zero-order paths on the circle, but it is a choice of a possible classical configuration, rather than an imposed constraint.

3.1 Hydrogen dianion

We estimate first the (approximate) thresholds for the appearance of the harmonic vibrational modes. If one takes $\frac{1}{5} \ll 1$, then it follows that for the case in hand ($Z = 1$) the above approximation holds for the lowest, ground state harmonic energy $m = 0$, if $L > 37.50$ and similarly, for $m = 1$ if $L > 137$. In our case the zero-energy is that of the electrons circling around the nucleus along the common circular orbit. Up to approximately $L = 38$ the total energy consists only of this rotational part. Starting from $L = 38$ we have the oscillatory energy superimposed over the rotational one. In Table 1 we present some of the system characteristic (classical) quantities.

We give the value for the half-life of the lowest ($n = 1$) level, though, of course, quantum-mechanically the state is stable (*i.e.* τ should be infinite). The first ($n =$ 1–4) levels are quoted for the sake of completeness, for the semiclassical theory does not apply to these states. We

Table 1. Semiclassical model for H^{2-} dianion. All quantities are in atomic units. $L_{\max}$ is the maximum system angular momentum quantum number, r_{eq} the single-electron equilibrium distance, λ_r is the Lyapunov exponent, τ is the level half-life, Ω is the system rotational angular frequency, ν and ω are the stability indices and vibrational angular frequencies, respectively. Number in parenthesis after a number denotes the power of 10 by which the number is to be multiplied.

$L_{\max}$	r_{eq}	λ_r	τ	Ω	ν_ϕ	ν_θ	$\omega_\phi/\omega_\theta$
1	0.5915	3.000	2.310(−1)	3.381	–	-	–
2	1.643	6.480(−1)	1.070	7.303(−1)	–	–	–
3	3.220	23.362(−1)	2.935	2.662(−1)	–	–	–
4	5.324	1.111(−1)	6.238	1.252(−1)	–	–	–
5	7.952	6.086(−2)	1.139(+1)	6.859(−2)	–	–	–
6	11.11	3.687(−2)	1.880(+1)	4.155(−2)	–	–	–
50	670.4	7.862(−5)	7.822(+3)	8.861(−5)	4.383	4.085	0.9320
150	5.955(+3)	2.970(−6)	2.070(+5)	3.348(−6)	4.383	4.085	0.9320
400	4.217(+4)	1.576(−7)	3.903(+6)	1.776(−7)	4.383	4.085	0.9320

Table 2. Rovibronic spectrum for H^{2-} dianion. All quantities are in atomic units. $L_{\max}$ is the system maximum angular momentum quantum number, E_0 is the zero-order system energy, ω and m are the vibrational angular frequencies and quantum numbers, respectively, and E_{tot} is the system total energy. Number in parenthesis after a number denotes the power of 10 by which the number is to be multiplied.

$L_{\max}$	$-E_0$	ω_ϕ	ω_θ	m_ϕ	m_θ	$-E_{\mathrm{tot}}$
1	1.072	2.359	2.198	–	–	1.072
2	1.286(−1)	5.095(−1)	4.748(−1)	–	–	1.286(−1)
3	6.562(−2)	1.857(−1)	1.73(−1)	–	–	6.562(−2)
4	3.970(−2)	8.735(−2)	8.141(−2)	–	–	3.970(−2)
5	2.657(−2)	4.784(−2)	4.459(−2)	–	–	2.657(−2)
6	1.903(−2)	2.899(−2)	2.701(−2)	–	–	1.903(−2)
50	3.152(−4)	6.181(−5)	5.761(−5)	0	0	2.555(−4)
150	3.549(−5)	2.254(−6)	2.176(−6)	0	0	3.327(−5)
150	3.549(−5)	2.254(−6)	2.176(−6)	1	0	3.102(−5)
150	3.549(−5)	2.254(−6)	2.176(−6)	0	1	3.109(−5)
150	3.549(−5)	2.254(−6)	2.176(−6)	1	1	2.884(−5)
250	1.281(−5)	4.889(−7)	4.720(−7)	0	0	1.233(−5)
250	1.281(−5)	4.889(−7)	4.720(−7)	1	0	1.184(−5)
250	1.281(−5)	4.889(−7)	4.720(−7)	0	1	1.186(−5)
250	1.281(−5)	4.889(−7)	4.720(−7)	1	1	1.137(−5)
250	1.281(−5)	4.889(−7)	4.720(−7)	2	1	1.088(−7)
250	1.281(−5)	4.889(−7)	4.720(−7)	1	2	1.090(−7)
250	1.281(−5)	4.889(−7)	4.720(−7)	2	2	1.041(−7)

note the large values of the half-life τ for the highly excited states. As mentioned above, this result appears both counter-intuitive and general. The frequency ratio (last column) is very close to the value one would obtain from the approximate formula (22) (0.9278).

We now calculate the energy spectrum of these rovibronic states. Formula (27), as it stands, requires solving an implicit equation with respect to the energy. In the case at hand (circular zero-order paths) it reduces practically to simply evaluating the rotational and vibrational parts separately and superimpose the latter on the former. In Table 2 we show part of the rovibronic spectrum for H^{2-}.

We notice that although the harmonic oscillatory modes are excited only after $L \approx 50$, unharmonic vibrations might exist below this limit. The corresponding spectrum in this region could be calculated from equations similar to equation (12), but with higher-order terms in the deviations included. We do not pursue, however, the

Table 3. The same as in Table 1 but for the semiclassical model for He$^-$ anion.

$L_{\max}$	r_{eq}	λ_r	τ	Ω	ν_ϕ	ν_θ	$\omega_\phi/\omega_\theta$
1	1.757(−1)	2.667(+1)	2.599(−2)	2.276(+1)	–	–	–
2	4.817(−1)	5.760	1.203(−1)	4.917	–	-	–
3	9.567(−1)	2.099	3.302(−1)	1.792	–	–	–
4	1.582	9.877(−1)	7.018(−1)	8.431(−1)	–	-	–
5	2.363	5.410(−1)	1.281	4.617(−1)	–	-	–
150	1.769(+3)	2.640(−5)	3.075(+4)	2.254(−5)	5.492	5.299	0.9649
400	1.253(+4)	1.401(−6)	5.796(+5)	1.196(−6)	5.491	5.299	0.9650

Table 4. The same as in Table 2 but for the rovibronic spectrum for He$^-$ anion.

$L_{\max}$	$-E_0$	ω_ϕ	ω_θ	m_ϕ	m_θ	$-E_{\text{tot}}$
1	4.048	–	–	–	–	4.048
2	1.457	–	–	–	–	1.457
3	7.435(−1)	–	–	–	–	7.435(−1)
4	4.498(−1)	–	–	–	–	4.498(−1)
5	3.011(−1)	–	–	–	–	3.011(−1)
150	4.021(−4)	1.627(−5)	1.901(−5)	0	0	3.845(−4)
400	5.678(−5)	1.045(−6)	1.009(−6)	0	0	5.575(−5)
400	5.678(−5)	1.045(−6)	1.009(−6)	1	0	5.471(−5)
400	5.678(−5)	1.045(−6)	1.009(−6)	0	1	5.475(−5)
400	5.678(−5)	1.045(−6)	1.009(−6)	1	1	5.370(−5)

investigations beyond the first-order perturbation theory here. Similarly, higher-order harmonics could be included for large L, too.

3.2 Helium anion

Similarly to the hydrogen dianion case, we estimate that for exciting zero-mode vibrations one has $L > 125$, and for $m = 1$ modes the condition $L > 375$. In Table 3 we show some of the system characteristic features.

As in the previous case, we notice good accuracy of the formula (22), which would yield 0.9639, instead of 0.9650 (see the last column in Table 3). By comparing the results for the hydrogen dianion (Table 1) and those in Table 3, one notices that the half-life decreases as the charge increases, although the stability indices increase (columns 4 and 6, 7). This is in accordance with formula (19), which together with equations (3,17) yields

$$\lambda_r \sim \left(\frac{Z}{L}\right)^3, \quad Z, L \gg 1, \tag{28}$$

The calculated spectrum has been shown in Table 4.

No experimental results or calculations have been reported on the triply highly excited helium anion. In [10] theoretical results for $n = 2$ triply excited states have been calculated. For $2p^3\,{}^2D^o$ the energy is $E = -0.7186$ au and estimated level width $\Gamma = 0.01036$ au, that corresponds to a half-life of 96.5 au. For $2s2p^2\,{}^2P$ $E = -0.7094$ au and $\tau = 344.5$ au (see, also, [23] and references therein). Clearly, disagreement with the semiclassical results, for both the energies (second column in Table 4) and half-lives (fourth column in Table 3), are enormous, as expected for these low-lying states.

3.3 Lithium atom

For the lithium atom ($Z = 3$) results are shown in Tables 5 and 6. We find, according to (24), the corresponding lower values for $L: 88\ (m = 0), 210\ (m = 1)$ and $438\ (m = 2)$.

Comparing numerical values for the stability indices in Tables 1, 3, 5, one sees that they change little with Z. Also, the frequences ratio (last column) appears close to one, even for this relatively small Z. This is another indication of the well-known fact that the electron mutual correlations diminish as the force exerted by the nucleus becomes stronger.

As for the experimental evidence, the situation appears similar to the helium case. In [33] the photon-induced transition in lithium $1s^22s(^2S) \to 2s^22p(^2P)$ has been observed, with $\Gamma \approx 0.20$ eV, that yields for the half-life $\tau \approx 136$ au, as compared with $4.395 \cdot 10^{-2}$ au in the fourth

Table 5. The same as in Table 1 but for the semiclassical model for Li atom.

$L_{\max}$	r_{eq}	λ_r	τ	Ω	ν_θ	ν_ϕ	$\omega_\phi/\omega_\theta$
1	1.032(−1)	7.301(+1)	9.493(−3)	5.814(+1)	–	–	–
2	2.866(−1)	1.577(+1)	4.395(−2)	1.256(+1)	–	–	–
3	5.618(−1)	5.747	1.206(−1)	4.577	–	–	–
4	9.287(−1)	2.704	2.563(−1)	2.153	–	–	–
5	1.387	1.481	4.680(−1)	1.179	–	–	–
100	4.632(+2)	2.428(−4)	2.855(+3)	1.933(−4)	5.646	5.783	0.9764
250	2.878(+3)	1.568(−5)	4.422(+4)	1.248(−5)	5.649	5.785	0.9764
500	1.148(+4)	1.965(−6)	3.527(+5)	1.565(−6)	5.649	5.781	0.9764

Table 6. The same as in Table 2 but for the rovibronic spectrum for Li atom.

$L_{\max}$	$-E_0$	ω_θ	ω_ϕ	m_θ	m_ϕ	$-E_{\mathrm{tot}}$
1	1.174(+1)	–	–	–	–	1.174(+1)
2	4.226	–	–	–	–	4.226
3	2.156	–	–	–	–	2.156
4	1.304	–	–	–	–	1.304
5	8.736(−1)	–	–	–	–	8.736(−1)
100	2.615(−3)	1.737(−4)	1.779(−4)	0	0	2.439(−3)
250	4.209(−4)	1.122(−5)	1.149(−5)	0	0	4.095(−4)
250	4.209(−4)	1.122(−5)	1.149(−5)	1	0	3.983(−4)
250	4.209(−4)	1.122(−5)	1.149(−5)	0	1	3.981(−4)
250	4.209(−4)	1.122(−5)	1.149(−5)	1	1	3.868(−4)
500	1.054(−4)	1.407(−6)	1.440(−6)	0	0	1.040(−4)
500	1.054(−4)	1.407(−6)	1.440(−6)	1	0	1.025(−4)
500	1.054(−4)	1.407(−6)	1.440(−6)	0	1	1.026(−4)
500	1.054(−4)	1.407(−6)	1.440(−6)	1	1	1.011(−4)
500	1.054(−4)	1.407(−6)	1.440(−6)	2	2	9.828(−5)

column of Table 5. The calculated energy $E_o = 150.28\,\mathrm{eV}$ of the resonance position corresponds to $E_2 = -1.955\,\mathrm{au}$, that is to be compared with $-4.226\,\mathrm{au}$ in column 2 in Table 6. We mention also the experimental results by Azuma *et al.* [34] on the photon-induced triply excited states of lithium. The experiment detected a great number of resonant states above the $2s^2 2p\,{}^2P^o$ resonance at 142.3 eV. Resonance structures have been attributed to mixtures of electronic configurations, which include states from $n = 2$ to $n = 5$. Obviously, if a comparison with semiclassical results is to be made, a more appropriate classification scheme must be adopted, as mentioned above.

4 Concluding remarks

We have calculated rovibronic spectra and stability indices for triply excited trielectronic systems, within the semiclassical plane model. For the lower states, which do not allow for the vibronic modes, only rotor-like kinematic is possible. For the sufficiently high excitations vibrational motion sets in. This is an atomic analogue to the polyatomic molecular semiclassical models, but based on the single-electron ansatz (see, *e.g.*, [46] and references therein for the collective coordinates quantization scheme). It should be noted here, however, that we have not treated our trielectronic system as a rigid rotator, unlike Herrick's approach [47], for in the Coulombic case one cannot speak of a rigid structure.

There are other possible classical configurations that may be used for the semiclassical calculations. One class of these structures would be isosceles triangles rotators (what would imply intershell states), with the rotational axis in the triangle plane (Langmuir-like rotator, see, *e.g.*, [8]). The same procedure used for the coplanar structure can be applied, and the rovibrational spectra derived.

In the low-lying levels case the semiclassical theory, at least within the model applied here, greatly underestimate both the energies and half-lives of these states. In the case of the energy estimates it is understandable, for the semiclassical model rests on the classical configuration which minimizes the electron potential, unlike the quantum-mechanical approach. As for the stability properties the simple semiclassical models are not capable to account for subtle effects, like wave function symmetry properties, which govern the transitions probabilities and thus determine the excited states half-lives. On the other hand, as the degree of excitation rises, these quantum-mechanical features tend to be smeared out and the semiclassical approach becomes both legitimate and increasingly accurate. It is, therefore, desirable that measurements of higher triple excitations, to $n \geq 5$, are carried out.

The classical radii of these highly excited states appear enormous by the ordinary standards within the atomic world, being of the order of $10^4\,a_o$. Such mesoscopic species are hardly observable under the standard laboratory conditions and may exist only in the interstellar space [19]. Since hydrogen and helium are the most abundant elements, the existence of their negative ions in the triply highly excited states may be detected *via* the corresponding radio emissions.

Present calculations may be extended to higher Z-values, but considering the above-mentioned conditions for detecting such states this extension does not appear appealing at the moment. On the other hand, extension to quadruply and even higher-multiplicity excited states could be made in a straightforward manner, within the present model. Because the latter is based on the balance between the attractive net Coulombic interaction and the centrifugal force, in the case of four electrons, for instance, the equilibrium configuration appears either a tetrahedral three-dimensional rotational structure, or rotational parallelograms. Of course, the restriction to rotating structures does not hold within the quantum-mechanical theory and the nonrotating tetrahedral configuration can be realized for $^5S^o$-symmetry, for example [48]. The present approach can be extended to nonrotating structures, like those indicated by Bao [3], as mentioned in the introduction. Although the total angular momentum may be small, even zero, individual electron angular momenta appear large close to the total ionization (fragmentation) threshold and the semiclassical theory is applicable.

Further possible extension of the model within the intrashell states would be the inclusion of the noncircular orbits, not very close to zero-eccentricity ellipses. The essence of the approach would not change, however, but one could no longer speak of a rovibrational structure, since the skeleton, zero-order configuration has no constant angular velocity and the electrons would execute a sort of breathing quasirotational motion.

I thank Dr. N. Simonović for the critical reading of the manuscript and for the assistance in preparing the compuscript. I am grateful to the referee for helpful remarks and suggestions. This work has been done under a partial support of the Ministry of Science and Technology of Serbia.

References

1. S. Watanabe, C.D. Lin, Phys. Rev. A **36**, 511 (1987).
2. W. Ruan, C.-G. Bao, Few Body Systems **14**, 25 (1993).
3. Cheng-guang Bao, Z. Phys. D **22**, 557 (1992).
4. Bao Cheng-guang, J. Phys. B **25**, 3725 (1992).
5. J. Leopold, I. Percival, J. Phys. B **13**, 1037 (1980).
6. M.S. Dimitrijević, P. Grujić, Fizika **17**, 1 (1985).
7. J.Müller, J. Burgdörfer, Phys. Rev. Lett. **17**, 2375 (1993).
8. C.G. Bao, W.F. Xie, C.D. Lin, J. Phys. B **27**, L193 (1994).
9. M. Bylicki, Phys. Rev. A **45**, 2079 (1992).
10. C. Nicolaides, N. Piangos, Y. Komninos, Phys. Rev. A **48**, 3578 (1993).
11. Y. Komninos, C. Nicolaides, Phys. Rev. A **50**, 3782 (1994).
12. A.Bürgers, N. Brandefeld, E. Lindroth, J. Phys. B **31**, 3181 (1998).
13. C. Nicolaides, M. Chrysos, Y. Komninos, Phys. Rev. A **41**, 5244 (1990).
14. P. Grujić, in *X European Symposium Dynamics of Few-Body Systems, Balatonfüred, 1986*, edited by Gy. Bencze, P. Doleshall, J. Reval (Budapest, 1986) pp. 253-281; M.S. Dimitrijević, P. Grujić, N. Simonović, Z. Phys. D **15**, 203 (1990).
15. H. Bachau, J. Phys. B **29**, 4365 (1996).
16. B. Gou, K. Chung, J. Phys. B **29**, 6103 (1996).
17. L.D. Landau, E.M. Lifshitz, *Quantum Mechanics* (Pergamon Press, Oxford, 1965).
18. A. Norcliffe, in *Case Studies in Atomic Physics*, edited by E. McDaniel, M. McDowell (North-Holland/American Elsevier, 1975) pp. 46-55.
19. I. Percival, Adv. Chem. Phys. **36**, 1 (1977).
20. D. Wintgen, K. Richter, G. Tanner, Chaos **2**, 19 (1992).
21. N. Simonović, P. Grujić, in *Proceedings of the Course Advances and Methods in the Study of Atomic Doubly Excited States*, edited by J. Mahecha, J. Botero (Universidad de Antioquia, Medellin, 1996) pp. 107-153.
22. M. Bylicki, C. Nicolaides, J. Phys. B **31**, L685 (1998).
23. J.M. Mercero, J.E. Fowler, C. Sarasola, J.M. Ugalde, Phys. Rev. A **57**, 2550 (1998).
24. B. Peart, K.T. Dolder, J. Phys. **6**, 1497 (1973).
25. T. Tanabe, I. Katayama, H. Kamegaya, K. Watanabe, Y. Arakaki, M. Yoshizava, Y. Haruyama, M. Saito, T. Honma, K. Hosono, K. Hatanaka, F.J. Curell, K. Noda, Phys. Rev. A **54**, 4069 (1996).
26. H. Hogreve, J. Phys. B **31**, L439 (1998).
27. T. Sommerfeld, U.V. Riss, H.-D. Meyer, L.S. Cederbaum, Phys. Rev. Lett. **77**, 470 (1996).
28. L. Vejby-Christensen, D. Kella, D. Mathur, H.B. Pedersen, H.T. Schmidt, L.H. Anderson, Phys. Rev. A **53**, 2371 (1996).
29. F. Robicheaux, R.P. Wood, C.H. Greene, Phys. Rev. A **49**, 1866 (1994).
30. T. Morishita, C.D. Lin, C.G. Bao, Phys. Rev. Lett. **80**, 464 (1998).
31. A.E. Klinkmüller, G. Haeffler, D. Hanstorp, I.Yu. Kiyan, U. Berzinsh, D.J. Pegg, J. Phys. B **31**, 2549 (1998).
32. E. Sokell, A.A. Wills, P. Hammond, M.A. MacDonald, M.K. Odling-Smee, J. Phys. B **29**, L863 (1996).
33. L.M. Kiernan, E.T. Kennedy, J.-P. Mosnier, J.T. Costello, Phys. Rev. Lett. **72**, 2359 (1994).
34. Y. Azuma, S. Hasegawa, P. Koike, G. Kuluk, T. Nagata, E. Shigemasa, A. Yagishita, I.A. Sellin, Phys. Rev. Lett. **74**, 3768 (1995).
35. P. Grujić, J. Phys. B **21**, 63 (1988).
36. Z. Gaeta, M. Noel, D. Stroud, Phys. Rev. Lett. **73**, 636 (1994).
37. P. Grujić, J. Phys. B **16**, 2567 (1983).
38. M. Poirier, Phys. Rev. A **40**, 3498 (1989).
39. P. Grujić, N. Simonović, Phys. Rev. A **50**, 4386 (1994).
40. N. Simonović, Phys. Rev. A **50** 4390 (1994).
41. S. Cvejanović, Z. Dohčević, P. Grujić, J. Phys. B **23**, L167 (1990).
42. P.V. Grujić, Bull. Astron. Belgrade, No. 152, 79 (1995); P. Grujić, J. Appl. Spectrosc. **63**, 831 (1996).
43. M. Chrysos, G. Aspromallis, Y. Komninos, C.A. Nicolaides, Phys. Rev. A **46**, 5789 (1992).
44. C. Nicolaides, Y. Komninos, J. Phys. B **19**, 1701 (1986); **23**, L571 (1990).
45. W.H. Miller, J. Chem. Phys. **63**, 996 (1975).
46. G. Ezra, C. Martens, L. Fried, J. Phys. Chem. **91**, 3721 (1987).
47. D. Herrick, Adv. Chem. Phys. **52**, 1 (1983).
48. C. Bao, Xiazhou Yang, C.D. Lin, Phys. Rev. A **55**, 4168 (1997).